Observed climatology and trend in relative humidity in the central and eastern Tibetan Plateau

Qinglong You, Jinzhong Min, Houbo Lin, Nick Pepin, Mika Sillanpää, Shichang K

Abstract

Monthly surface relative humidity (RH) data for 71 stations in the Tibetan Plateau (TP) provided by the National Meteorological Information Center/China Meteorological Administration are compared with corresponding grid points from the National Center for Environmental Prediction/National Center for Atmospheric Research (NCEP/NCAR hereafter) reanalysis. Mean climatologies, interannual variabilities, and trends calculated by the Mann-Kendal method are analyzed during 1961–2013. The annual regional long-term mean surface RH is 55.3%, with a clear maximum in summer (66.4%) and minimum in winter (44.9%). Compared with observations, NCEP/NCAR overestimates RH in all seasons, especially in spring (18.2%) and winter (17.8%). Mean annual regional surface RH has decreased by -0.23%/decade and even more rapidly in summer (-0.60%/decade) and autumn (-0.39%/decade). The reduction of surface RH is also captured by the NCEP/NCAR reanalysis at the surface, 400, 500, and 600 hPa. A particularly sharp reduction of RH since the mid-1990s is evident in both data sets, in line with rapid warming over the plateau. This suggests that moisture supply to the plateau from the Arabian Sea and the Bay of Bengal is limited and that variability and trends of surface RH over the TP are not uniquely driven by the Clausius-Clapeyron relationship.

1. Introduction

Relative humidity (RH) is the ratio of the partial pressure of water vapor to the saturation vapor pressure of water at the same temperature [Intergovernmental Panel on Climate Change (IPCC), 2013]. RH directly affects atmospheric visibility and has a strong influence on the formation of clouds, fog, and smog [Elliott and Angell, 1997; Van Wijngaarden and Vincent, 2005]. RH also regulates evapotranspiration, thus being a critical control of hydrological processes (including precipitation, condensation, and evaporation) and surface energy budgets [Gaffen and Ross, 1999]. Changes and variations in RH in the lower levels of the atmosphere are critical to understanding changes in the hydrological cycle, including moisture content and precipitation. Thus, understanding patterns and trends in RH will reduce uncertainties in the estimation of future climatic changes [Van Wijngaarden and Vincent, 2005; Vicente-Serrano et al., 2014; Xie et al., 2011].

In recent decades, significant progress has been made in the analysis of RH through multiple data sets. Using the analysis of the European Centre for Medium-Range Weather Forecasts Re-Analyses (ERA-40 and ERA-Interim), a widespread reduction in RH has occurred over land, which may be due to limited moisture supply from the oceans [Simmons et al., 2010]. On regional scales, comprehensive analyses have improved understanding, modeling, and prediction of RH [Isaac and Van Wijngaarden, 2012; Simmons et al., 2010]. In the U.S. during 1961–1995 [Gaffen and Ross, 1999], RH shows slight positive trends. This conclusion has been confirmed over a longer period (1930–2010) [Brown and DeGaetano, 2013] using a newly constructed data set. In Canada [Van Wijngaarden and Vincent, 2005], RH decreased during 1953–2003 in the west, especially in winter and spring, which corresponded with rapid warming. These studies are consistent with results across North America during 1948–2010 [Isaac and Van Wijngaarden, 2012]. A similar reduction in RH has been reported from subregional studies in Europe, including southern Spain [Espadafor et al., 2011] and the whole of the country [Vicente-Serrano et al., 2014]. Based on radiosonde stations in China during 1979–2005 [Xie et al., 2011], annual and seasonal trends in RH at 850 hPa, 700 hPa, and 500 hPa were insignificant in most regions. However, Xinjiang/central China showed upward/downward trends, consistent with previous studies [Wang and Gaffen, 2001]. On a global scale, Dai [2006] examined surface data from over 15,000 weather stations and ships during 1975–2004 and showed that RH increased by 0.5% to 2% per decade over the central and eastern United States, India, and western China. In each case, this was associated with an increase in temperature, low clouds, and specific humidity [Dai, 2006].

The Tibetan Plateau (TP) is the highest and most extensive highland area in the world and has been called the “Third Pole” and the “Asian Water Tower” [Kang et al., 2010]. The TP is the origin of several large Asian rivers, including the Yangtze, Yellow River, Salween, and Mekong, which supply more than one billion people of China and other downstream countries [Yao et al., 2012]. Thus, moisture availability over the plateau is of critical importance. Due to its height, the plateau also plays a major role in the formation of summer circulation through the heating of its elevated surface. This thermal influence also interacts with the development of weather systems over east China and boreal climate patterns more generally [Duan and Wu, 2005, 2009; Wu et al., 2014]. Recent studies have pointed to the TP region’s unique sensitivity to rapidly changing climate and changing emissions of gas phase and aerosol pollutants in Asia [Fu et al., 2006; Li et al., 2005]. This region also hosts one of the most complex meteorological and observing environments in the world [Duan and Wu, 2005; Kang et al., 2010]. Understanding the sensitivity of this region to changes in climate and air quality requires observations that can help answer questions of how weather, climate, dynamics, and radiative processes are linked. For example, the summertime anticyclone over the TP has

been considered important to Asian pollution trapping and outflow [Li et al., 2005]; sounder storms over the TP provided a pathway for water vapor and trace gases transport to the global stratosphere [Fu et al., 2006]. Moreover, numerous prior studies have illustrated rapid climate and cryospheric change in the TP using observational stations, reanalyses, and remotely sensed data [Kang et al., 2010; Rangwala, 2013; Yao et al., 2012; You et al., 2008a]. RH is also critical to understanding the changing hydrosphere and cryosphere, including ablation of glaciers and development of cloud/precipitation. However, there is a lack of observations describing recent surface climatology, variability, and trends in RH in the TP. Here we present long-term climatological and seasonal surface RH distributions(winter: December-January-February (DJF), spring: March-April-May (MAM), summer: (June-July-August) JJA, and autumn: September-October-November (SON)) in the TP for 1961–2013 using a new surface data set and evaluate trends in surface RH over the same period.

2. Data and Methods

Monthly surface relative humidity (RH) data for 71 stations in the TP are provided by the National Meteorological Information Center/China Meteorological Administration (NMIC/CMA) (Figure 1). There are 156 stations in the original data. A total of 124 stations maintain daily data since 1961; of these stations, 38 stations are excluded owing to the elevation below 2000m above sea level (asl), then 12 stations are also excluded owing to problems in data. The distribution of the stations is uneven and very sparse in the western TP, which may influence the regional trends. Therefore, 3 stations in the western TP are also excluded. The remaining 71 stations with elevation above 2000m asl were selected [You et al., 2008a, 2008b]. Most stations are in the eastern and central TP (mostly Qinghai and Tibet) and were installed in the 1950s. All are above 2000m above sea level (asl), and individual elevations range from 2109.5m to 4700m asl. The same data set has been analyzed for variability and trends in other meteorological elements, including temperature and precipitation extremes [Kang et al., 2010; You et al., 2008a, 2008b].

Monthly means of surface RH from the National Center for Environmental Prediction/National Center for Atmospheric Research (NCEP/NCAR hereafter) reanalysis are provided by NOAA/Office of Oceanic and Atmospheric Research (OAR)/Earth System Research Laboratory Physical Sciences Division (ESRL PSD), Boulder, Colorado, USA, from http://www.cdc.noaa.gov/. The data set covers January 1948 to the present day with 4 times daily data available at 00:00, 06:00, 12:00, and 18:00 universal time coordinated [Kalnay et al., 1996; Kistler et al., 2001]. Upper air RH is represented by monthly means at 300, 400, 500, and 600 hPa. The 71 grid points nearest to the observation stations (Figure 1) are derived from NCEP/NCAR with the linear interpolation methods to identify the comparison. Since

much data are missing before 1960, we selected the period of 1961–2013 for analysis. The Mann-Kendall test has been popularly used to assess the significance of trend in time series. The test requires sample data to be serially independent. When sample data are serially correlated, the presence of serial correlation in time series will affect the ability of the test to correctly assess the significance of trend. So in this paper, the Mann-Kendall test for trends and Sen's slope estimates are used to detect and estimate trends in annual and seasonal RH [Sen, 1968], with significance defined as $P<0.05$.

3. Results

3.1. Spatial and Temporal Variations of Surface RH From Observations and NCEP/NCAR

Figures 2 and 3 show spatial patterns of annual and seasonal mean surface RH from the 71 surface stations and NCEP/NCAR, respectively, during 1961–2013. Long-term climatological means for surface RH on an annual and seasonal basis are summarized in Table 1. The regional annual mean surface RH (average of the 71 stations) is 55.3%, with a clear maximum in summer (66.4%) and minimum in winter (44.9%) (Table 1). These values are higher than previous studies in high terrain such as the Rocky Mountains have shown [Dai, 2006]. The annual mean surface RH has maximum values in the southeastern TP (more than 80%) and minimum values (lower than 40%) in the north-west (Figure 2). The decrease from south-east to north-west is consistent with the distribution of total cloud cover [You et al., 2014]. In summer, the spatial distribution of mean surface RH is similar to in other seasons, but high values in the south-east illustrate the influence of the Asian monsoon system. The south-east remains the most humid region in all other seasons except winter (Figure 2).

For NCEP/NCAR, the regional annual mean surface RH is 69.8%, with maximum/minimum values in summer/winter (77.2%/62.7%) (Table 1). These values significantly overestimate observations by an average of 14.5% on an annual basis. Overestimations occur in all seasons but especially in spring (18.2%) and winter (17.8%) (Table 1). Despite overestimation, the spatial distribution of mean surface RH is largely in agreement with observations (Figure 3). The distributions of surface RH from NCEP/NCAR reveal that RH is also strongly controlled by the evolution and variability of the monsoon system.

3.2. Trends in Surface RH From Observations and NCEP/NCAR

Figures 4 and 5 show spatial patterns in trends of annual and seasonal surface RH from surface stations and NCEP/NCAR, respectively, during 1961–2013. Positive trends are shown as upward triangles and negative trends as downward triangles. The size of the triangle is proportional to trend magnitude. Figure 6 presents a time series of the regional annual and seasonal mean RH from all surface stations versus NCEP/NCAR during 1961–2013. Annual

and seasonal trend statistics are listed in Table 1, and the number of increasing/decreasing trends is summarized in Table 2.

On an annual basis, the mean regional surface RH series from observations decreases slowly up until the mid-1980s and after a slight recovery shows a sharp decrease after 2005. Over the whole period, RH has decreased by 0.23%/decade, although this does not pass the significance level (Table 1). Forty-seven individual stations however show a decrease in surface RH, and the trend is significant at 22 of them. Stations in the central TP tend to have larger trend magnitudes, which corresponds with analyses of downward trends in total cloud cover [You et al., 2014]. On a seasonal basis, the highest rate of RH decrease occurs in summer (-0.60%/decade), significant at $P<0.01$, and 62 stations show a downward trend. Rates for spring, autumn, and winter are -0.11, -0.39, and -0.04%/decade, respectively, but only autumn is statistically significant. The majority of stations (>40 in all seasons) shows decreasing trends (Table 2).

For NCEP/NCAR reanalysis, decreasing trends also predominate. The regional mean surface RH series decreases from 1961 to 2013 at -0.32%/decade, passing the significance level $P<0.01$ (Table 1). Forty-five grid points have negative trends for surface RH, and 23 grid points show significance at $P<0.05$. Stations in the south-west have larger trend magnitudes, which are slightly inconsistent with the observations. On a seasonal basis, the strongest decreases occur in spring (-0.54%/decade), and rates for summer, autumn, and winter are -0.08, -0.41 and -0.20%/decade, respectively. Similar to the annual picture, the majority of stations (>45) shows a significant decreasing trend in all seasons (Table 2).

Similar to observations, the surface RH from NCEP/NCAR therefore exhibits reducing trends but often with larger trend magnitudes. In contrast, the largest trends differ in season, and there are discrepancies in the seasonal variation in trend patterns between data sets.

3.3. Trends in RH in the TP From NCEP/NCAR at 300 hPa, 400 hPa, 500 hPa, and 600 hPa

Figure 7 shows the spatial patterns of trends of annual and seasonal RH from NCEP/NCAR at 500 hPa for the same period. Figure 8 presents regional anomalies of annual and seasonal RH from NCEP/NCAR at 300, 400, 500, and 600 hPa. Trend magnitudes of annual and seasonal RH from NCEP/NCAR at the same pressure levels are summarized in Table 3. On an annual basis, the mean RH from NCEP/NCAR at all pressure levels shows a significant downward trend during 1961–2013, especially after 2000, resulting in regional trends of -0.10, -1.08, and -0.70%/decade for 400, 500, and 600 hPa, respectively. The RH at 500 hPa in particular demonstrates significant negative trends in most regions (Figure 7), especially in

the central southern part of the plateau around 31°N, 96°E. RH at 300 hPa on the other hand has been increasing with a rate of 0.27%/decade (Table 3). On a seasonal basis, the steepest decreases at 400 hPa and 500 hPa have occurred in spring (-0.43 and -1.63%/ decade) ($P<0.05$), while at 600 hPa, this has been in winter (-1.05%/decade). Summer declines have actually been slight in comparison with other seasons (Table 3).

4. Discussion and Conclusions

Surface RH in the TP from observations and from NCEP/NCAR reanalysis has been compared. At the majority of observing stations, surface RH has reduced during 1961–2013, particularly in summer (-0.60%/decade) and autumn (-0.39%/decade). NCEP/NCAR reanalysis shows the strongest declines in spring and autumn (-0.54 and -0.41%/decade, respectively).The lowest annual values are recorded around 2010, which has resulted from a rapid reduction since the mid-1990s. This is consistent with global patterns reported by Simmons et al. [2010], who showed that an abrupt decrease in RH occurred over land areas in the last decade. In Europe, a large decrease in mean annual RH has been reported in Poland [Wypych, 2010], the Czech Republic [Brázdil et al., 2009; Cahynová and Huth, 2009], and Spain [Vicente-Serrano et al., 2014]. For the Greater Alpine Region [Brunetti et al., 2009], the large decreases in RH in recent decades have mostly been associated with summer patterns. The reduction of surface RH we report in the TP is also consistent with trends observed over the mainland of China [Wang and Gaffen, 2001; Xie et al., 2011], even though some earlier analyses showed contrasting results [Dai, 2006]. Dai [2006] showed large positive RH trends (0.5–2.0% decade_1) over western China and most of East Asia in all seasons. Trends of surface RH have been shown to vary with study period and data set, including differences between weather stations [Dai, 2006] and Hadley Centre and Climatic Research Unit Global Surface Humidity (HadCRUH) [Simmons et al., 2010; Willett et al., 2008]. Despite this, our results showing an abrupt decrease in RH are consistent with most observations made in other regions of Europe and the mainland of China over recent decades (see Table 4 for a comparison of our results with other studies).

The reduction of surface RH is also confirmed by the NCEP/NCAR reanalysis [Kalnay et al., 1996; Kistler et al. 2001]. RH at the surface, and all pressure levels at 400 hPa and below, shows downward trends over the whole TP and is positively correlated with the observations. Despite the overall agreement, there are seasonal differences in trends with NCEP/NCAR having weaker trends in summer and stronger trends in winter and spring, inconsistent with observations (Table 3). It is unclear therefore whether short-scale variability of RH in the TP can be reproduced entirely from NCEP/NCAR reanalysis. RH from NCEP/NCAR overestimates that of observations in the TP, but overall, RH does show a reduction during

1961–2013 in both data sets, also corresponding with ERA-Interim and Japanese 25-year Reanalysis on a global scale [Simmons et al., 2010].

The reduction of surface RH is associated with a significant increase of minimum, maximum, and mean temperatures during the same period in the TP [You et al., 2008a]. According to the Fifth Assessment Report of the Intergovernmental Panel on Climate Change, the globally averaged combined land and ocean surface temperature shows a warming of 0.85 (0.65–1.06)°C over the period of 1880–2012 [IPCC, 2013]. Under global warming, the TP has experienced particularly rapid warming during the last half century, and it is projected to continue at a faster rate than the global mean [Kang et al., 2010]. The negative correlation (R = 0.44 for observation and R =_0.40 for NCEP/NCAR reanalysis) between surface RH and temperature has been revealed by this study (Figure 6), in contrast with the previous studies that the RH declines a little as temperature increases. The pronounced decline in RH over the plateau is consistent with a limited moisture supply from the oceans [Simmons et al., 2010]. In summer, the TP is strongly influenced by the strong Indian monsoon, which brings abundant moisture evaporated from the Arabian Sea and the Bay of Bengal [Kang et al., 2010; Yao et al., 2012]. Thus, how surface RH is reacting to the evolution and variability of the monsoon system remains unclear. According to the Clausius-Clapeyron relationship, the atmosphere could store more moisture with the increase of temperature. But this is not the case for the TP. Actually the observed RH is reduced with the increase of temperature over TP. The only explanation is that the sharp reduction of RH suggests a limited moisture supply in the atmosphere. Thus, it is also suggested that variability and trends of surface RH in the TP are not uniquely driven by the Clausius-Clapeyron relationship, which determines how much moisture the atmosphere can hold.

This is confirmed by another study in Spain [Vicente-Serrano et al., 2014]. Further investigation of the mechanisms responsible for RH changes is desirable but beyond the scope of this study. Long-term trends in surface RH are associated with many processes, including temperature change, precipitation changes, atmospheric circulation patterns, and even anthropogenic factors [IPCC, 2013; Simmons et al., 2010; Xie et al., 2011]. Further studies need to focus on quantifying the effect of each factor and its contribution to the reduction of surface RH observed in the TP.

Acknowledgments. This study is supported by the State Key Program of National Natural Science Foundation of China (41230528), National Natural Science Foundation (91437216 and 41201072); Jiangsu Specially-Appointed Professor (R2013T07), Jiangsu Natural Science Funds for Distinguished Young Scholar “BK20140047”, Open Research Fund Program of Plateau Atmosphere and Environment Key Laboratory of Sichuan Province (PAEKL-2014-K1) and the Priority Academic Program Development of Jiangsu Higher Education Institutions

(PAPD). Observations are provided by the National Meteorological Information Center, China Meteorological Administration (NMIC/CMA) （http://cdc.cma.gov.cn/home.do), and NCEP/NCAR reanalysis is provided by NOAA/OAR/ESRL PSD, Boulder, Colorado, USA, from their website at http://www.cdc.noaa.gov/. We are very grateful to the reviewers for their constructive comments and thoughtful suggestions.

References

Brázdil, R., K. Chromá, P. Dobrovolný, and R. Tolasz (2009), Climate fluctuations in the Czech Republic during the period 1961–2005, Int. J. Climatol., 29(2), 223–242.

Brown, P. J., and A. T. DeGaetano (2013), Trends in U.S. surface humidity, 1930–2010, J. Appl. Meteorol. Climatol., 52(1), 147–163.

Brunetti, M., G. Lentini, M. Maugeri, T. Nanni, I. Auer, R. Boehm, and W. Schoener (2009), Climate variability and change in the Greater Alpine Region over the last two centuries based on multi-variable analysis, Int. J. Climatol., 29(15), 2197–2225.

Butler, C., and A. García-Suárez (2012), Relative humidity at Armagh Observatory, 1838–2008, Int. J. Climatol., 32(5), 657–668.

Cahynová, M., and R. Huth (2009), Changes of atmospheric circulation in central Europe and their influence on climatic trends in the Czech Republic, Theor. Appl. Climatol., 96(1–2), 57–68.

Dai, A. (2006), Recent climatology, variability, and trends in global surface humidity, J. Clim., 19(15), 3589–3606.

Duan, A. M., and G. X. Wu (2005), Role of the Tibetan Plateau thermal forcing in the summer climate patterns over subtropical Asia, Clim. Dyn., 24(7–8), 793–807, doi:10.1007/s00382-004-0488-8.

Duan, A. M., and G. X. Wu (2009), Weakening trend in the atmospheric heat source over the Tibetan Plateau during recent decades. Part II: Connection with climate warming, J. Clim., 22(15), 4197–4212, doi:10.1175/2009jcli2699.1.

Elliott, W. P., and J. K. Angell (1997), Variations of cloudiness, precipitable water, and relative humidity over the United States: 1973–1993, Geophys. Res. Lett., 24(1), 41–44, doi:10.1029/96GL03616.

Espadafor, M., I. Lorite, P. Gavilán, and J. Berengena (2011), An analysis of the tendency of reference evapotranspiration estimates and other climate variables during the last 45 years in southern Spain, Agric. Water Manage., 98(6), 1045–1061.

Fu, R., Y. Hu, J. S.Wright, J. H. Jiang, R. E. Dickinson, M. Chen, M. Filipiak, W. G. Read, J.W.Waters, and D. L.Wu (2006), Short circuit of water vapour and polluted air to the global stratosphere by convective transport over the Tibetan Plateau, Proc. Natl. Acad. Sci. U.S.A., 103(15), 5664–5669.

Gaffen, D. J., and R. J. Ross (1999), Climatology and trends of U.S. surface humidity and temperature, J. Clim., 12(3), 811–828.

Intergovernmental Panel on Climate Change (IPCC) (2013), Summary for Policymakers of Climate Change 2013: The Physical Science Basis. Contribution of Working Group I to the Fifth Assessment Report of the Intergovernmental Panel on Climate Change, Cambridge Univ. Press, Cambridge, U. K.

Isaac, V., and W. Van Wijngaarden (2012), Surface water vapor pressure and temperature trends in North America during 1948–2010, J. Clim., 25(10), 3599–3609.

Kalnay, E., et al. (1996), The NCEP/NCAR 40 year reanalysis project, Bull. Am. Meteorol. Soc., 77(3), 437–471.

Kang, S. C., Y. W. Xu, Q. L. You, W. A. Flugel, N. Pepin, and T. D. Yao (2010), Review of climate and cryospheric change in the Tibetan Plateau, Environ. Res. Lett., 5(1), 015101, doi:10.1088/1748-9326/5/1/015101.

Kistler, R., et al. (2001), The NCEP-NCAR 50 year reanalysis: Monthly means CD-ROM and documentation, Bull. Am. Meteorol. Soc., 82(2), 247–267.

Li, Q., J. H. Jiang, D. L. Wu, W. G. Read, N. J. Livesey, J. W. Waters, Y. Zhang, B. Wang, M. J. Filipiak, and C. P. Davis (2005), Convective outflow of South Asian pollution: A global CTM simulation compared with EOS MLS observations, Geophys. Res. Lett., 32, L14826, doi:10.1029/2005GL022762.

Rangwala, I. (2013), Amplified water vapour feedback at high altitudes during winter, Int. J. Climatol., 33(4), 897–903.

Sen, P. K. (1968), Estimates of regression coefficient based on Kendall's tau, J. Am. Stat. Assoc., 63, 1379–1389.

Simmons, A., K. Willett, P. Jones, P. Thorne, and D. Dee (2010), Low-frequency variations in surface atmospheric humidity, temperature, and precipitation: Inferences from reanalyses and monthly gridded observational data sets, J. Geophys. Res., 115, D01110, doi:10.1029/ 2009JD012442.

Van Wijngaarden,W. A., and L. A. Vincent (2005), Examination of discontinuities in hourly surface relative humidity in Canada during 1953–2003, J. Geophys. Res., 110, D22102, doi:10.1029/2005JD005925.

Vicente-Serrano, S. M., C. Azorin-Molina, A. Sanchez-Lorenzo, E. Morán-Tejeda, J. Lorenzo-Lacruz, J. Revuelto, J. I. López-Moreno, and F. Espejo (2014), Temporal evolution of surface humidity in Spain: Recent trends and possible physical mechanisms, Clim. Dyn., 42(9–10), 2655–2674.

Wang, J. X., and D. J. Gaffen (2001), Late-twentieth-century climatology and trends of surface humidity and temperature in China, J. Clim., 14(13), 2833–2845.

Willett, K. M., P. D. Jones, N. P. Gillett, and P. W. Thorne (2008), Recent changes in surface humidity: Development of the HadCRUH data set, J. Clim., 21(20), 5364–5383.

Wu, G., A. Duan, Y. Liu, J. Mao, R. Ren, Q. Bao, B. He, B. Liu, and W. Hu (2014), Recent progress in the study of Tibetan Plateau climate dynamics, Natl. Sci. Rev., doi:10.1093/nsr/nwu045.

Wypych, A. (2010), Twentieth century variability of surface humidity as the climate change indicator in Kraków (Southern Poland), Theor. Appl. Climatol., 101(3–4), 475–482.

Xie, B., Q. Zhang, and Y. Ying (2011), Trends in precipitable water and relative humidity in China: 1979–2005, J. Appl. Meteorol. Climatol., 50(10), 1985–1994, doi:10.1175/2011jamc2446.1.

Yao, T. D., et al. (2012), Different glacier status with atmospheric circulations in Tibetan Plateau and surroundings, Nat. Clim. Change, 2(9), 663–667, doi:10.1038/nclimate1580.

You, Q. L., S. C. Kang, E. Aguilar, and Y. P. Yan (2008a), Changes in daily climate extremes in the eastern and central Tibetan Plateau during 1961–2005, J. Geophys. Res., 113, D07101, doi:10.1029/2007JD009389.

You, Q. L., S. C. Kang, N. Pepin, and Y. P. Yan (2008b), Relationship between trends in temperature extremes and elevation in the eastern and central Tibetan Plateau, 1961–2005, Geophys. Res. Lett., 35, L04704, doi:10.1029/2007GL032669.

You, Q. L., Y. Jiao, H. Lin, J. Min, S. Kang, G. Ren, and X. Meng (2014), Comparison of NCEP/NCAR and ERA-40 total cloud cover with surface observations over the Tibetan Plateau, Int. J. Climatol., 34, 2529–2537.

Figures

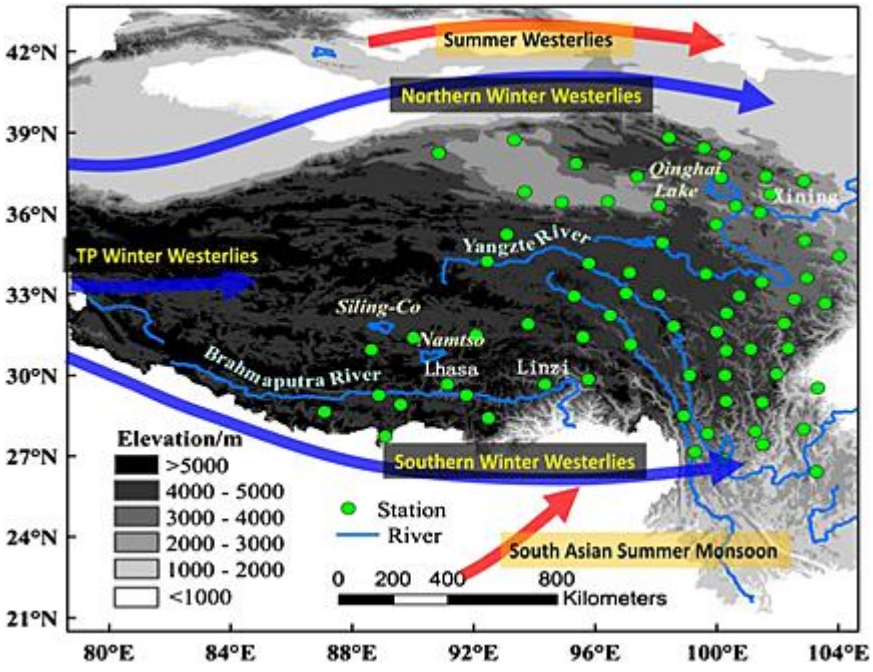

Figure 1. Distribution of 71 surface stations (white dots) in the Tibetan Plateau.

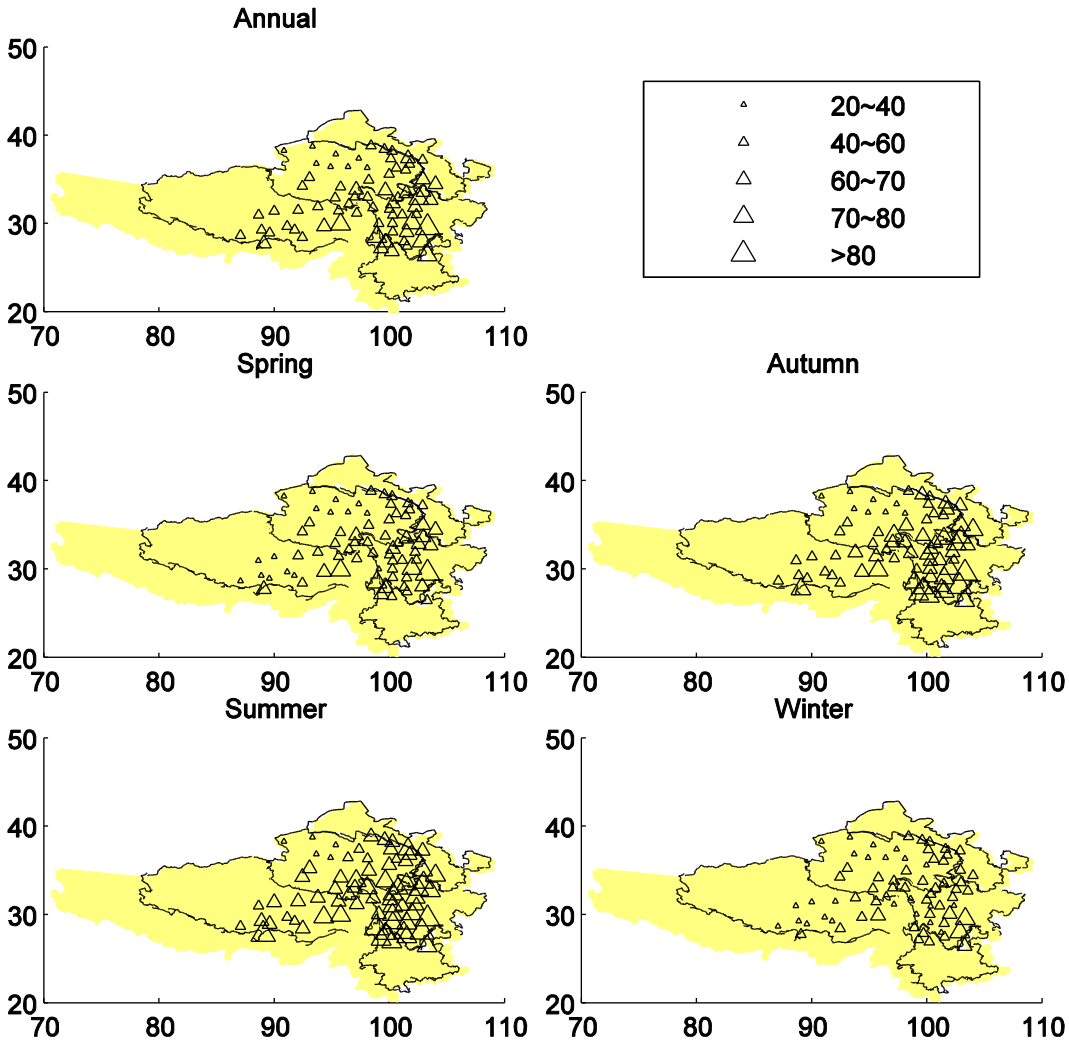

Figure 2. Spatial patterns of annual and seasonal mean relative humidity from 71 surface stations in the Tibetan Plateau during 1961-2013. The size of the dot is proportional to the magnitude of the mean values. The unit is %.

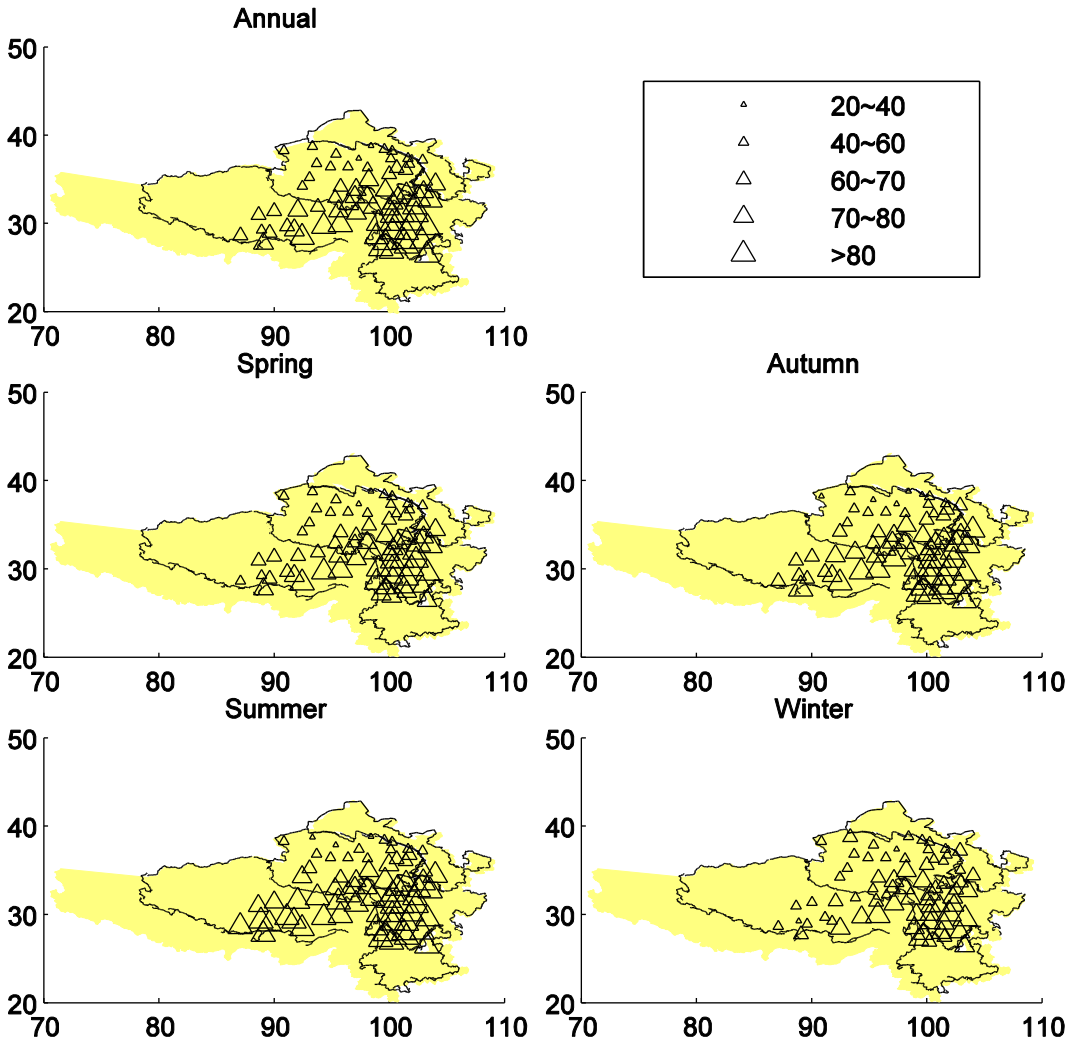

Figure 3. Spatial patterns of annual and seasonal mean relative humidity from NCEP/NCAR in the Tibetan Plateau during 1961-2013. Positive trends are shown as up triangle, negative trends as down triangle. The size of the triangle is proportional to the magnitude of the trends. The trends are calculated by the Mann-Kendal methods and the trends with the significant level are marked. The unit is % per decade.

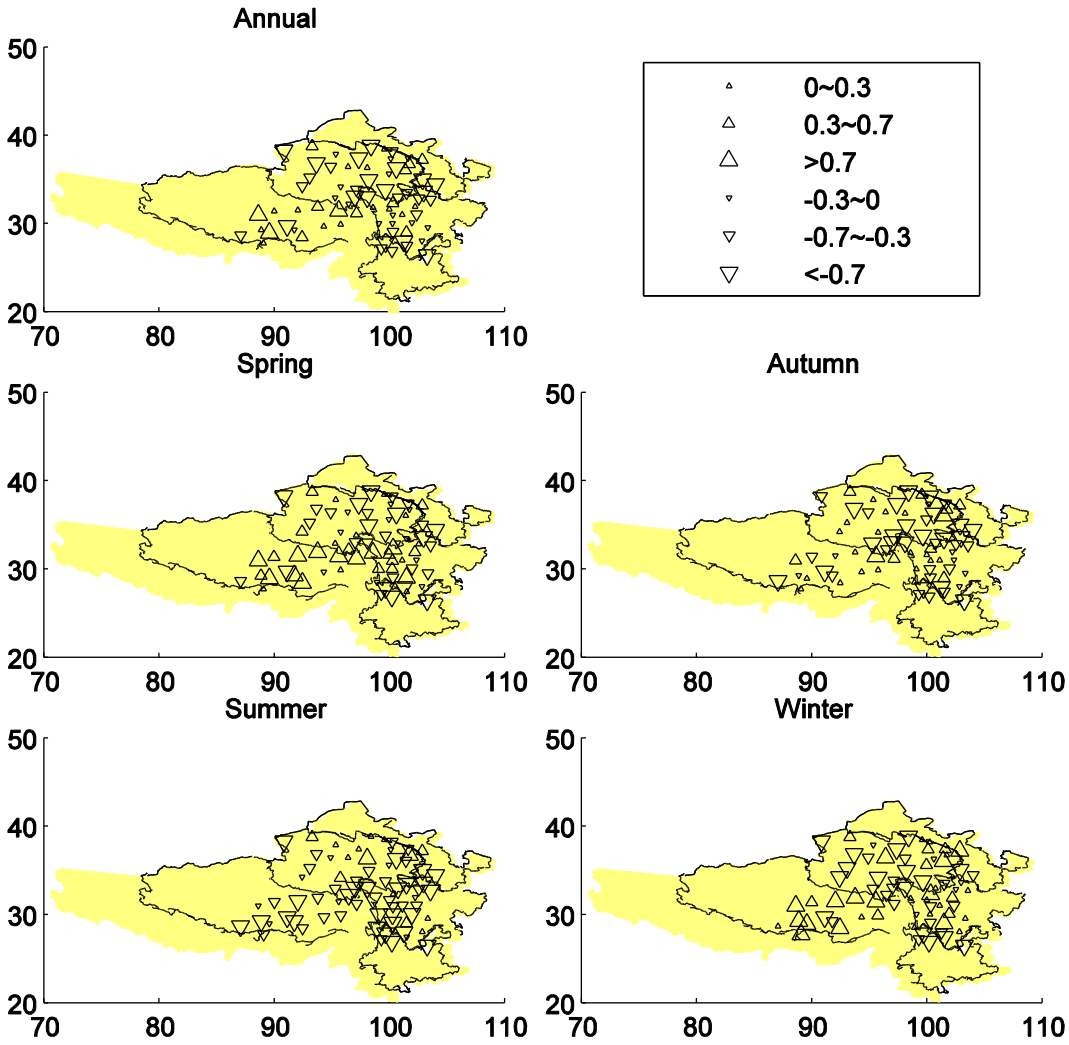

Figure 4. Spatial patterns of trends of annual and seasonal relative humidity from 71 surface stations in the Tibetan Plateau during 1961-2013. Other is same as Figure 3.

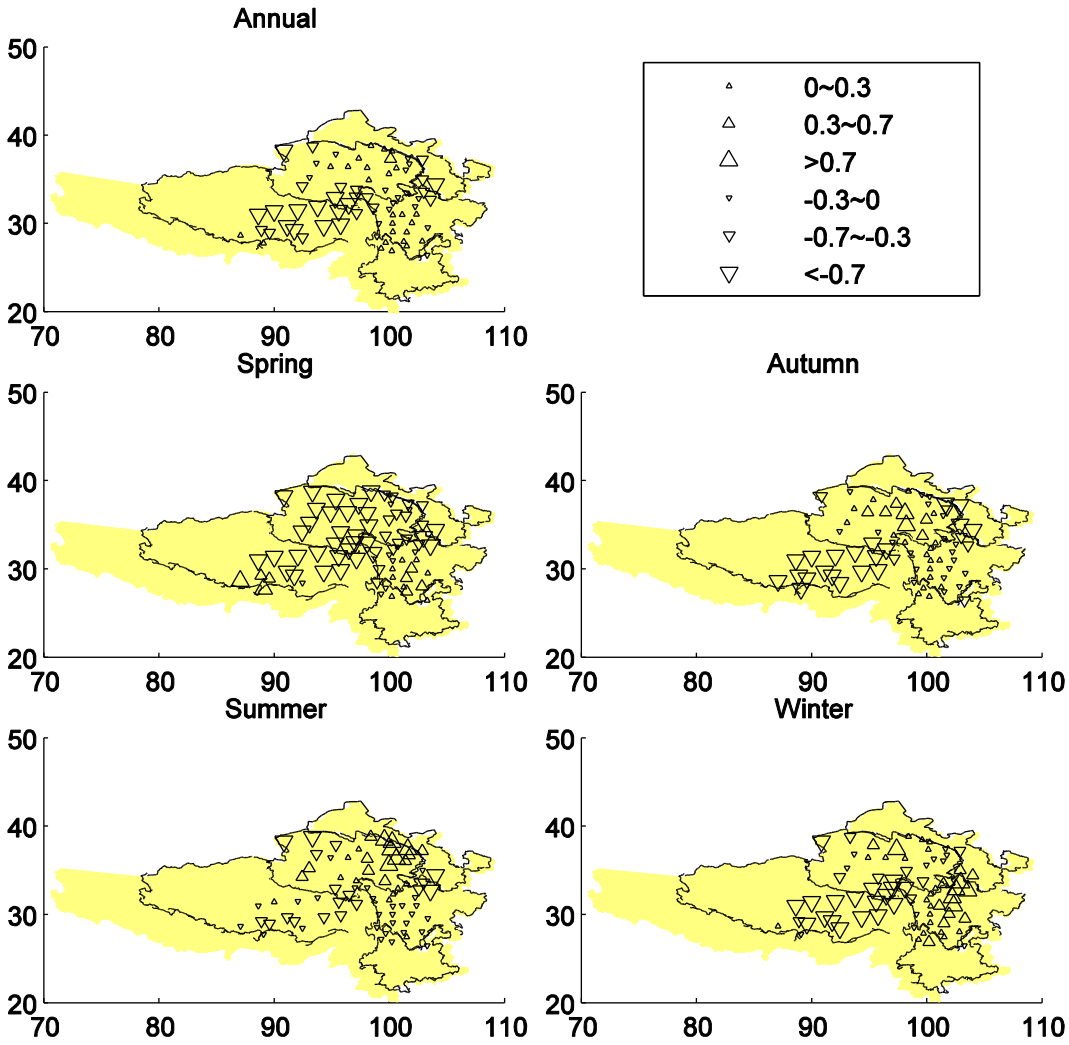

Figure 5. Spatial patterns of trends of annual and seasonal relative humidity from NCEP/NCAR in the Tibetan Plateau during 1961-2013. Other is same as Figure 3.

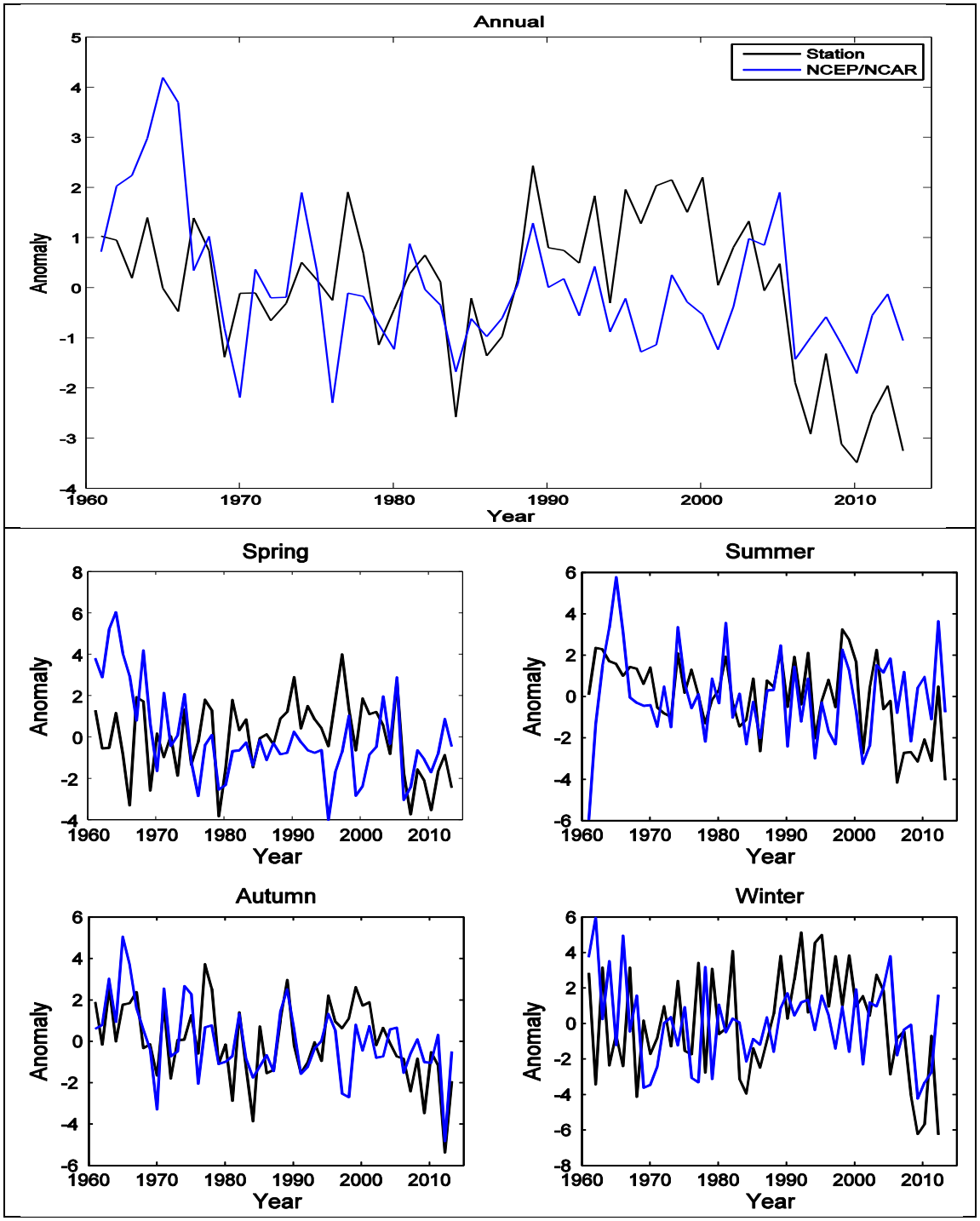

Figure 6. Regional anomaly of relative humidity from surface stations and NCEP/NCAR on the annual and seasonal basis in the Tibetan Plateau during 1961-2013.

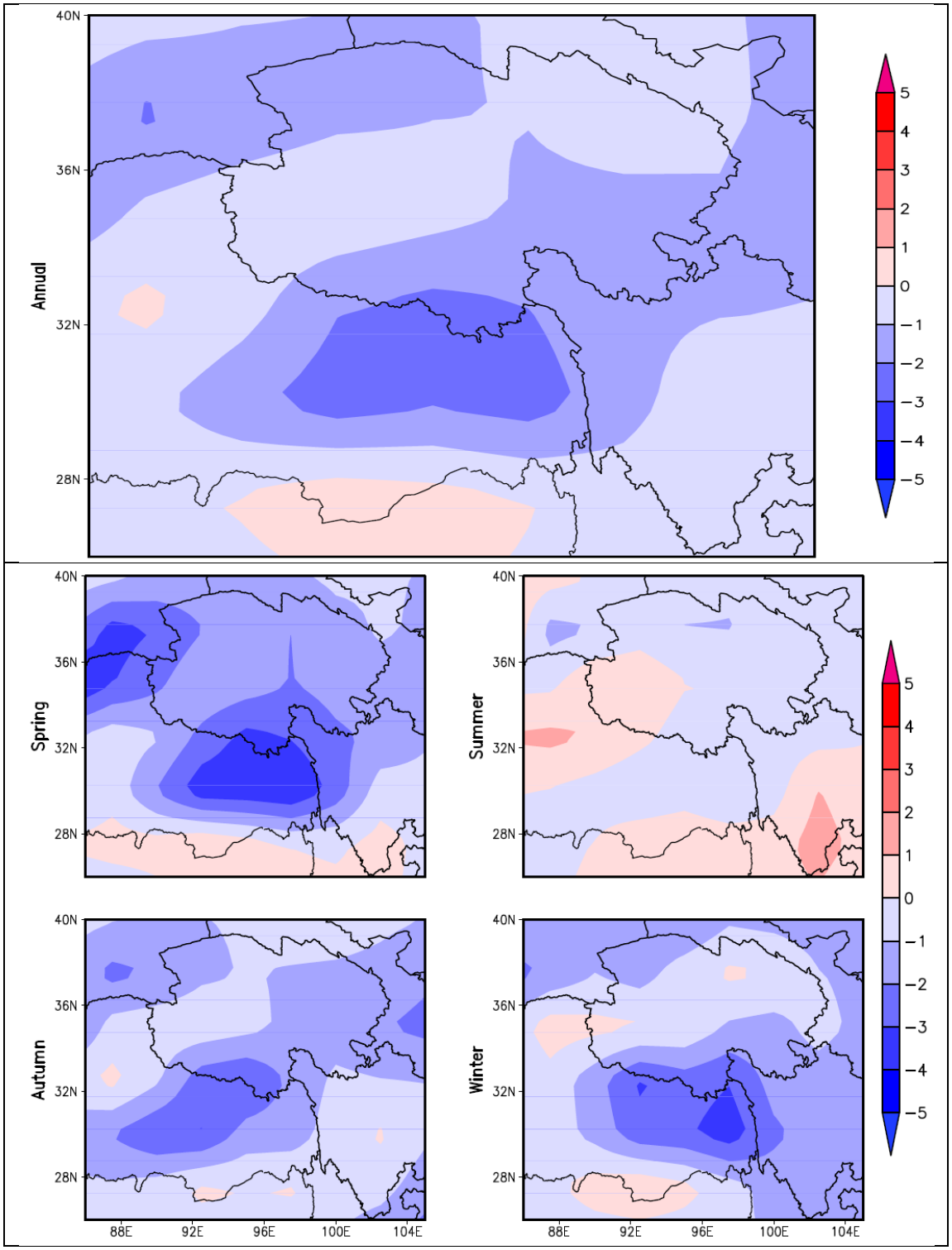

Figure 7. Spatial patterns of trends of relative humidity from NCEP/NCAR at 500 hPa in the Tibetan Plateau on the annual and seasonal basis during 1961-2013.

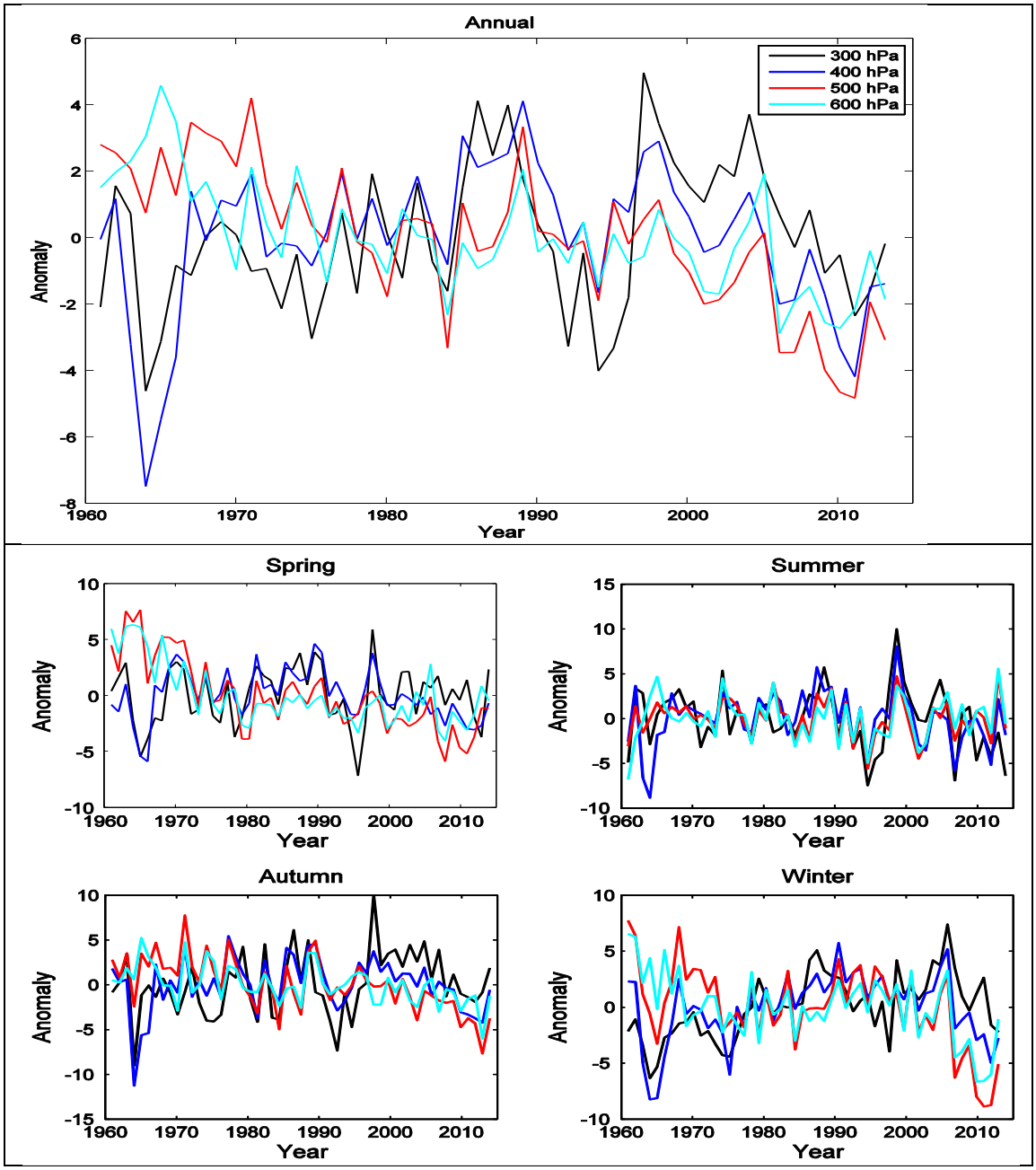

Figure 8. Regional anomaly of relative humidity from NCEP/NCAR at 300 hPa, 400hPa, 500 hPa and 600 hPa in the Tibetan Plateau on the annual and seasonal basis during 1961-2013.

Tables

Table 1. Annual and seasonal mean surface relative humidity and trends in the eastern and central Tibetan Plateau during the period of 1961-2013. The trends with a significance level greater than 95% are highlighted in mark. Unit is % for mean value and % decade^{-1} for trend, respectively.

	Annual	Spring	Summer	Autumn	Winter
Mean value (%)					
Observation	55.3	49.9	66.4	60.1	44.9
NCEP/NCAR	69.8	68.1	77.2	71.3	62.7
NCEP/NCAR-Observation	14.5	18.2	10.8	11.2	17.8
Trend (% decade^{-1})					
Observation	-0.23	-0.11	-0.60**	-0.39**	0.04
NCEP/NCAR	-0.32**	-0.54**	-0.08	-0.41**	-0.20

** Significant at the 0.05 level; * Significant at the 0.1 level

Table 2. The number of increase/decrease trends of surface relative humidity from the surface stations and NCEP/NCAR in the Tibetan Plateau on the annual and seasonal basis during 1961-2013. The number of stations with a significance level greater than 95% are shown in parentheses.

		Annual	Spring	Summer	Autumn	Winter
Observation	Increase	24(7)	26(6)	9(3)	17(3)	31(8)
	Decrease	47(22)	45(11)	62(33)	54(18)	40(12)
NCEP/NCAR	Increase	26(0)	16(4)	25(4)	25(0)	34(7)
	Decrease	45(23)	55(31)	46(12)	46(25)	37(18)

Table 3. Trends of annual and seasonal relative humidity from NCEP/NCAR at 300 hPa, 400hPa, 500 hPa and 600 hPa in the Tibetan Plateau during 1961-2013. The trends with a significance level greater than 95% are highlighted in mark. Unit is % decade^{-1}, respectively.

	Annual	Spring	Summer	Autumn	Winter
300 hPa	0.27	0.11	-0.40	0.50	1.01**
400 hPa	-0.10	-0.43*	-0.18	-0.15	0.35
500 hPa	-1.08**	-1.63**	-0.19	-1.21**	-1.30**
600 hPa	-0.70**	-1.02**	0	-0.63**	-1.05**

** Significant at the 0.05 level; * Significant at the 0.01 level

Table 4. Summary of trends of relative humidity on the regional and global scales in recent decades.

Region	Dataset	Period	Trend (%/decade)	Reference
U.S	170 stations	1961-1995	Slight increase	Gaffen and Ross, 1999
U.S	175 stations	1930-2010	Annual:0.27 DJF: 0.705 MAM:0.403 JJA:0.036 SON:0.193	Brown and DeGaetano, 2013
Canada	75 stations	1953-2003	Decrease	Van Wijngaarden and Vincent, 2005
North America	309 stations	1948-2010	-0.5	Isaac and Van Wijngaarden, 2012
Southern Spain	8 stations	1960-2005	-0.01- -0.23	Espadafor et al., 2011]
Spain	868 stations	1961-2011	Annual:-1.02 DJF: -0.66 MAM:-1.02 JJA:-1.56 SON:-0.83	Vicente-Serrano et al., 2014
Poland	1 station	1901-2000	Decline	Wypych, 2010]
Czech Republic	23 stations	1961-2005	Decline	Brázdil et al., 2009
Czech Republic	21 stations	1961-1998	Decline	Cahynová and Huth, 2009
Northern Ireland	1 station	1838-2008	Annual:0.11 DJF: -0.01 MAM:0.17 JJA:0.18 SON:0.10	Butler and García‐Suárez, 2012
Alpine region	242 stations	1880-2005	Slight decrease	Brunetti et al., 2009
China	196 stations	1951-1994	Decrease	Wang and Gaffen, 2001
China	106 radiosonde stations	1979-2005	No significant trends	Xie et al., 2011
Global	15000 weather stations	1976-2005	-0.09	Dai, 2006
Global (only land)	HadCRUH	1973-2008	Decrease	Simmons et al., 2010]
Global	HadCRUH	1973-2003	-0.10	Willett et al., 2008